Remote Sensing of Environment 242 (2020) 111744

Contents lists available at ScienceDirect

Remote Sensing of Environment

journal homepage: www.elsevier.com/locate/rse

# Temporal variability of GNSS-Reflectometry ocean wind speed retrieval performance during the UK TechDemoSat-1 mission

Matthew Lee Hammond*, Giuseppe Foti, Christine Gommenginger, Meric Srokosz

*National Oceanography Centre, Southampton, SO14 3ZH, UK*

ARTICLE INFO

Edited by Menghua Wang

*Keywords:*
Global Navigation Satellite System (GNSS)
GNSS Reflectometry (GNSS-R)
GNSS remote sensing
TechDemoSat-1 (TDS-1)
Ocean remote sensing
Ocean wind speed
Attitude
GPS flex mode

ABSTRACT

This paper presents the temporal evolution of Global Navigation Satellite System Reflectometry (GNSS-R) ocean wind speed retrieval performance during three years of the UK TechDemoSat-1 (TDS-1) mission. TDS-1 was launched in July 2014 and provides globally distributed spaceborne GNSS-R data over a lifespan of over three years, including several months of 24/7 operations. TDS-1 wind speeds are computed using the NOC Calibrated Bistatic Radar Equation algorithm version 0.5 (C-BRE v0.5), and are evaluated against ERA5 high resolution re-analysis data over the period 2015–2018. Analyses reveal significant temporal variability in TDS-1 monthly wind speed retrieval performance over the three years, with the best performance (~2 $m{\cdot}s^{-1}$) achieved in the early part of the mission (May 2015). The temporal variability of retrieval performance is found to be driven by several non-geophysical factors, including TDS-1 platform attitude uncertainty and spatial/temporal changes in GPS transmit power from certain satellites. Evidence is presented of the impact of the GPS Block IIF Flex mode on retrieved GNSS-R wind speed after January 2017, which results in significantly underestimated ocean winds over a large region covering the North Atlantic, northern Indian Ocean, the Mediterranean, the Black Sea, and the Sea of Okhotsk. These GPS transmit power changes are shown to induce large negative wind speed biases of up to 3 $m{\cdot}s^{-1}$. Analyses are also presented of the sensitivity of TDS-1 wind speed retrieval to platform attitude uncertainty using statistical simulations. It is suggested that a 4° increase in attitude uncertainty can produce up to 1 $m{\cdot}s^{-1}$ increase in RMSE, and that TDS-1 attitude data do not fully reflect actual platform attitude. We conclude that the lack of knowledge about the GNSS-R nadir antenna gain map and TDS-1 platform-attitude limits the ability to determine the achievable wind speed retrieval performance with GNSS-R on TDS-1. The paper provides recommendations that accurate attitude knowledge and a good characterisation of GNSS-R nadir antenna patterns should be prioritised for future GNSS-R missions.

## 1. Introduction

Global Navigation Satellite System Reflectometry (GNSS-R) is an innovative and rapidly developing approach to Earth Observation (EO) that makes use of signals of opportunity from Global Navigation Satellite Systems (GNSS), which have been reflected from the Earth's surface. This idea was first proposed in the late 1980s (Hall and Cordey, 1988), before the first practical detection and development to provide geographic information over a wide array of surfaces in the 2000s (e.g. Komjathy et al., 2000; Gleason, 2006). The technology uses a bistatic scattering configuration based on signals from GNSS transmitters that are forward scattered off the surface of the Earth; a detailed overview of the mechanisms and physics of GNSS-R can be found in Zavorotny et al. (2014). Dedicated GNSS-R receivers placed on platforms such as the UK TechDemoSat-1 (TDS-1) satellite are used to detect and correlate reflected GNSS signals with the original or local replica of the direct signals from the same GNSS transmitter. Examining the correlation between the reflected and direct signals allows inference of geophysical information about the Earth surface, such as the reflectivity, roughness, or elevation. The technology is particularly promising as it does not require a dedicated transmitter, thereby reducing cost, mass, and power requirements of the receivers. These advantages offer the potential to deploy GNSS-R sensors as affordable multi-satellite constellations (e.g. Carreno-Luengo et al., 2016) or as payloads of opportunity aboard other missions. The technology also offers the possibility of improvements in the future by virtue of the large and increasing number of GNSS transmitting satellites from multiple systems (including GLONASS, BeiDou, Galileo etc.) which should increase the number of simultaneous reflections available across the GNSS-R receiver field-of-view. Combining signals from as many of these GNSS systems as possible offers the

* Corresponding author.
*E-mail address:* matthew.hammond@noc.ac.uk (M.L. Hammond).

https://doi.org/10.1016/j.rse.2020.111744
Received 11 July 2019; Received in revised form 28 January 2020; Accepted 28 February 2020
Available online 24 March 2020

opportunity of a sustainable low-cost Earth Observation system with high spatial resolution and coverage and significantly better temporal sampling than present-day satellites. Another advantage of GNSS-R is the use of L-band microwave signals (~20 cm wavelength) which are less sensitive to atmospheric attenuation by atmospheric water vapour and precipitation than other higher frequency microwave sensors, allowing for better wind estimates under heavy rain, including in hurricane conditions (Foti et al., 2017a).

A large number of applications of GNSS-R have been successfully demonstrated in previous studies, including: ocean surface roughness and wind speed (see e.g. Komjathy et al., 2004; Katzberg et al., 2006; Gleason and Gebre-Egziabher, 2009; Foti et al., 2015), lake surface topography (e.g. Li et al., 2018), oil slicks (e.g. Valencia et al., 2011), tsunamis (e.g. Yan and Huang, 2016a), soil moisture (e.g. Masters et al., 2000; Camps et al., 2018), vegetation biomass (Egido et al., 2014), sea-ice (e.g., Yan and Huang, 2016b; Alonso-Arroyo et al., 2017), and land ice elevation mapping (Cartwright et al., 2018). The successful launch by Surrey Satellite Technology Ltd. of the UK TechDemoSat-1 (TDS-1) mission in July 2014, and its quasi-continuous operation since launch, has delivered a unique dataset of globally distributed spaceborne GNSS-R data, spanning a period of four years, that has been used to provide evidence of the benefits of GNSS-R for global environmental monitoring.

This paper focuses once again on GNSS-R for ocean winds, but specifically for the first time, considers the temporal evolution of TDS-1 ocean wind speed retrieval performance over 3 years based on a single consistent methodology. Many studies have previously estimated the quality of ocean wind speeds retrieved with TDS-1 data (e.g. Foti et al., 2015; Soisuvarn et al., 2016; Foti et al., 2017a, 2017b; Asgarimehr et al., 2018) using a number of inversion algorithms, performance metrics, and means of validation applied to different subsets of TDS-1 data. Overall, TDS-1 wind retrievals based on Signal to Noise Ratio (SNR) report acceptable performance relative to scatterometers, buoys, and reanalysis models, but with marked differences in reported errors. Since TDS-1 GNSS-R signals are affected also by non-geophysical factors, notably platform attitude uncertainty, ambient noise hotspots (Foti et al., 2017b), and GPS transmitter power, it is informative to examine how the TDS-1 wind retrieval performance, estimated with one consistent inversion and validation methodology, varies geographically and temporally through the lifetime of the mission.

This paper presents the GNSS-R ocean wind speed retrieval performance of TDS-1 estimated at monthly intervals over 3 years. TDS-1 wind speeds are obtained using the National Oceanography Centre (NOC) Calibrated Bistatic Radar Equation (C-BRE) inversion algorithm and validated against ERA5 reanalysis data (Section 2). For the first time, the variability of the TDS-1 wind retrieval performance is examined over different regions and different periods of the TDS-1 mission (Section 3). The approach establishes a clear link between the TDS-1 wind retrieval performance and changes in platform attitude and GPS transmit power. Statistical simulations confirm the sensitivity of TDS-1 wind retrieval performance to platform attitude uncertainty (Section 4), leading to important recommendations for future GNSS-R missions (Section 5).

## 2. Data and methods

### 2.1. TDS-1 mission and GNSS-R data

TDS-1 was launched successfully on the 8th of July 2014. The satellite was placed into a Low Earth Orbit with a nominal altitude of 635 km and an inclination of 98.4°. The orbit is quasi-sun synchronous with a local time of ascending node drift of 1.42 h per year. The platform attitude control is driven with an onboard Kalman filter, which uses inputs from a magnetometer and multiple sun sensors.

The TDS-1 mission carries eight experimental payloads, including a GNSS-R prototype receiver known as the Space GNSS Receiver Remote Sensing Instrument (SGR-ReSI) which has been operational since September 2014. The SGR-ReSI is a small, low mass, low power receiver based on commercial off-the-shelf components to improve cost effectiveness, and thus enable potential widespread use. Full details of the instrument and platform can be found in Jales and Unwin (2015).

The SGR-ReSi collects reflected signals using a highly directional downward pointing antenna, with a peak gain of 13.3 dBi and a half-beamwidth of 15° (3 dB). The antenna main lobe points 6° from the platform nadir. The peak antenna gain is located behind the satellite until October 2016, when the satellite was rotated 180° in yaw in order to balance temperatures in the platform, after which date, the main lobe is pointing 6° in front of the satellite. The instrument is able to track, record and process reflected signals simultaneously from up to four different transmitters, with an on-board ranking process that allows the four strongest reflected signals to be selected based on estimated gain of the antenna at the specular point. Delay Doppler Maps (DDMs) are continuously generated onboard and posted at a frequency of 1 Hz, using a coherent integration time of 1 ms, followed by a 1-second incoherent accumulation. Level 1b DDM data from the TDS-1 SGR-ReSI are disseminated freely through the MERRByS web portal (www.merrbys.co.uk).

As a technology demonstration mission, the satellite originally operated an 8-day acquisition cycle where the SGR-ReSI operated only 2 out of every 8 days. This acquisition cycle ended in July 2017, when operations were temporarily suspended due to ground segment constraints. Operations of the satellite resumed in late October 2017, with the SGR-ReSI as the sole operational instrument and GNSS-R acquisitions taken 24 h a day, 7 days a week (24/7). The SGR-ReSI was switched off in December 2018, when TDS-1 formally reached end-of-life, in preparation for the deployment of the onboard de-orbiting sail.

At the start of the mission, the SGR-ReSI operated in unmonitored automatic gain mode (AGM) until the end of April 2015, when it switched to programmed gain mode (PGM) to allow radiometric calibration of the reflected signals. Large fluctuations are observed in DDM noise power in time and space (Foti et al., 2017b) and this effect is partially mitigated in AGM mode. However, radiometric calibration is not feasible when the receiver operates in AGM as the gain is unmonitored, thus limiting the retrieval to the use of uncalibrated SNR as an observable. The NOC C-BRE inversion algorithm operates on radiometrically calibrated reflected signals (see below). Therefore, the wind speed retrievals presented in this paper only relate to TDS-1 data from the end of April 2015, when the receiver started to operate in PGM. Fig. 1 shows the volume of valid data available over the ocean during the PGM period between April 2015 and August 2018 that is considered in this paper.

### 2.2. NOC C-BRE wind speed algorithm

The NOC C-BRE algorithm inverts wind speed from the DDM peak SNR, taking into account the bistatic geometry and the antenna gain at the specular point according to the Bistatic Radar Equation. The SNR used as the observable is defined as the ratio of the DDM power in the Signal and the Noise boxes in the DDM. The Noise power box (N) is fixed in DDM space and of constant size, covering all Doppler frequency bins and the first four delay (1 chip) bins in the signal free area of the DDM. The Signal box (S) also has a constant size of four delay bins and three Doppler bins (1 chip and 1500 Hz respectively), which corresponds to an average ground resolution of 25 km depending on the elevation angle of the specular point. Due to the fluctuations of the signal peak position within the DDM, the Signal box is positioned dynamically using an automatic detection approach following the application of a noise mitigation filter (Foti et al., 2015).

The Geophysical Model Function (GMF) of the NOC C-BRE inversion was derived using collocations with MetOp A/B ASCAT scatterometers during the early part of the TDS-1 mission, when the phasing of the TDS-1 drifting orbit provided a relatively high number of matchups

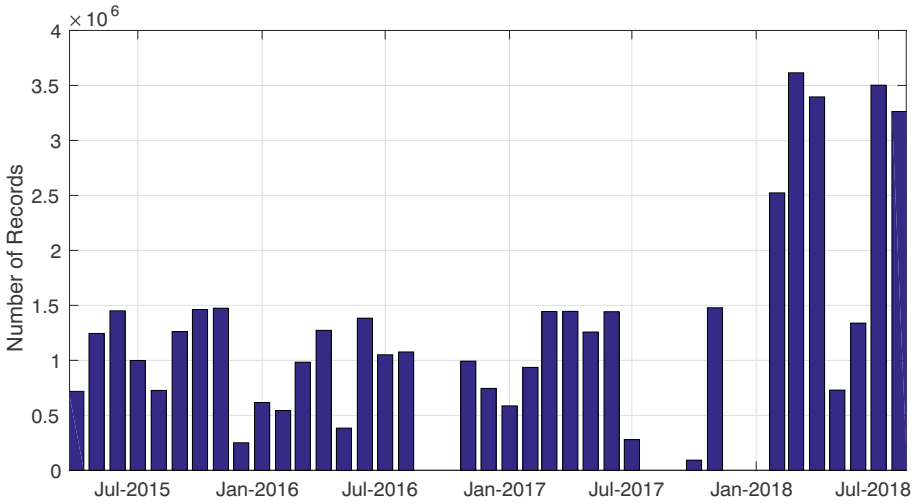


**Fig. 1.** Counts per calendar month of valid TDS-1 SGR-ReSI 1 Hz records over ocean during the TDS-1 Programmed Gain Mode (PGM) phase. Note that after October 2017 TDS-1 data are recorded 24 h a day and 7 days a week leading to the large increase in available data for ocean surface wind speed estimation.

within 0.5° and 1 h of the two ASCAT sensors. The inversion strategy additionally includes L1 calibration and correction modules based on time-invariant empirical corrections (i.e. computed once for the whole PGM period) that account for system, instrument, and geometry related biases. One of these corrections mitigates differences in direct signal power across GNSS transmitters, while another mitigates some of the errors linked to inaccuracies in the knowledge of the effective nadir antenna pattern aboard TDS-1.

The NOC C-BRE v0.5 algorithm applies only to ice-free open-ocean conditions, and the algorithm merely applies a rudimentary latitudinal mask between latitudes of 55°N and 55°S to reduce the effect of contamination by sea-ice. Due to the absence of a proper sea-ice flagging mechanism, typically strong returns from ice infested areas may be erroneously interpreted by the algorithm as unrealistically low ocean wind speeds. Although retrieval of ocean wind speeds has been demonstrated even in hurricane conditions when sufficient SNR is achieved (Foti et al., 2017a), there is insufficient collocated TDS-1/ASCAT data at high winds to reliably determine the GMF, resulting in greater uncertainty in GNSS-R winds in this range. For this reason, TDS-1 wind speed retrieval is capped at 20 $m{\cdot}s^{-1}$ in this version of the algorithm. Wind speed data retrieved using the NOC C-BRE v0.5 algorithm for TDS-1 SGR-ReSI are available freely as L2 products from the MERRByS web portal (www.merrbys.co.uk).

### 2.3. ERA5 re-analysis data

As explained, the NOC C-BRE algorithm was trained using collocations with ASCAT in the early phase of the mission when the local time of ascending node (LTAN) of TDS-1 was favourable to producing a sufficiently high number of close matchups. However, due to TDS-1 LTAN drift, the number of close matchups has reduced steadily over time, making collocated measurements with ASCAT scatterometers unsuitable for assessing the performance of TDS-1 winds consistently over the full mission lifespan. In fact, from early 2016, almost no coincident collections are available that satisfy the required collocation criteria between TDS-1 and MetOp A/B.

In order to analyse the performance of the C-BRE v0.5 algorithm over the length of the TDS-1 PGM period (April 2015 – August 2018), wind speed output from the ECMWF ERA5 reanalysis dataset is used (obtained from apps.ecmwf.int/data-catalogues/era5). ERA5 is a global climate reanalysis product combining models with observations, available over the period from 1979 until near present (the ERA5 hindcast data are released to the public with a latency of ~2–3 months). The ERA5 dataset is available in two forms: a reduced resolution ten-member ensemble known as the Ensemble of Data Assimilations (EDA), which provides uncertainty estimates; and a high-resolution realisation (HRES). For the assessment of the C-BRE v0.5 winds, the HRES product is used, due to its higher resolution. The HRES atmospheric data have a spatial resolution of 31 km and a temporal resolution of 1 h, versus a spatial resolution of 62 km and a temporal resolution of 3 h in the EDA product. The ERA5 products are shown to have negligible drift in fit with observations over time, and favourable spatial performance (Hersbach et al., 2018; Belmonte Rivas and Stoffelen, 2019). The ERA5 atmospheric variables include a number of surface wind parameters, of which the 10-metre $u$ and $v$ components of the surface wind vector are used in the assessment of the TDS-1 winds. Finally, the ERA5 data were collocated with TDS-1 specular point locations using the nearest grid point in space and time, which corresponds to a maximum spatial offset of half a grid cell (15.5 km) and a maximum temporal offset of 30 min.

## 3. Comparisons of TDS-1 wind speed with ERA5

### 3.1. Overall performance during the TDS-1 PGM period

The NOC C-BRE v0.5 algorithm performance is analysed over the global ocean, excluding wind speeds that are > 20 $m{\cdot}s^{-1}$ (which make up < 1% of the collocated ERA5 data), as well as high-latitude (> 55°) regions outside of the algorithm validity range. The overall performance across the whole mission (PGM) of TDS-1 winds compared to ERA5 is shown in Fig. 2. The validation plot shows that the highest density of wind speeds (~2–5 $m{\cdot}s^{-1}$) is generally being slightly underestimated by the C-BRE. This appears to be associated with the effect of a negative bias found later in the mission (see Section 3.2) together with a significantly higher volume of data acquisitions then. A small number of wind speeds above 10 $m{\cdot}s^{-1}$ are overestimated, mainly because of the asymmetric dependence of wind speed on SNR in this range, where a small decrease in SNR gives a greater positive wind speed bias than an equivalent increase in SNR (e.g. Foti et al., 2015).

### 3.2. Performance over time

The TDS-1 wind speed performance (bias, RMSE) is now examined on a monthly basis for the whole PGM period, considering separately data acquired in the eclipsed and sunlit parts of the orbit (when attitude uncertainties are larger – see Foti et al., 2017b). From Fig. 3, the wind speed retrieval performance does not appear to be stable over time. Best performance is obtained at the start of the PGM phase where RMSE is about 1.9 $m{\cdot}s^{-1}$ for data in eclipse during April 2015, albeit with a

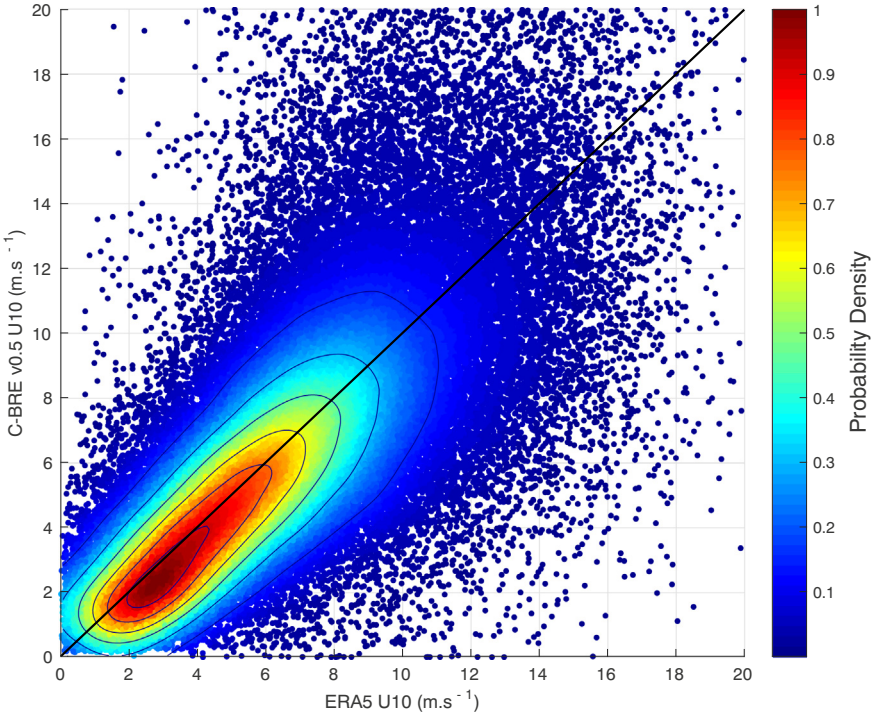


**Fig. 2.** Comparison of TDS-1 GNSS-R wind speed computed with the NOC C-BRE v0.5 algorithm against ERA5 reanalysis 10 metre wind speed over the open ocean between [55°N-55°S] latitude. Data are from the period April 2015 – August 2018. Colours and contour lines indicate the density of observations. (For interpretation of the references to colour in this figure legend, the reader is referred to the web version of this article.)

small positive bias. Following April 2015, and prior to the yaw manoeuvre in October 2016, the RMSE gradually increases over time, reaching a maximum of 3.3 m·s$^{-1}$ (in eclipse) in December 2016. The yaw manoeuvre in October 2016, i.e. when the platform was rotated 180° in yaw, has a significant effect on both RMSE and bias. Although the worst performance shortly follows the yaw manoeuvre, which could be attributable to instability of platform parameters following this procedure, inversion performance does subsequently improve, with RMSE again reaching 1.9 m·s$^{-1}$ (in eclipse) in October 2017 before stabilising around 2.5 m·s$^{-1}$ (in eclipse) up to August 2018. Likewise, the yaw manoeuvre affects the wind speed bias which becomes more negative following the manoeuvre. The sunlit and eclipse biases are also more similar for the entirety of 2017, although they appear to be drifting apart again in 2018. These fluctuations are thought to originate in part from changing attitude performance through the life of TDS-1. These and other possible causes of these variations are explored in Section 4 below.

### 3.3. Performance in geographical space

A global map of 1° gridded performance is presented in Fig. 4 that shows performance using the metric Relative Root Mean Square Error (RRMSE), defined as the RMSE divided by the average ERA5 wind speed in that grid cell, to indicate performance independent of wind speed distributions across the globe. Performance is shown to be best in the Southern Hemisphere with decreases in performance in the higher latitude Northern Hemisphere.

Spurious effects can be seen in three seas across the globe, specifically: Hudson Bay, the Labrador Sea, and the Sea of Okhotsk. Retrieved wind speeds are found to be unrealistically low in winter (Fig. 5)

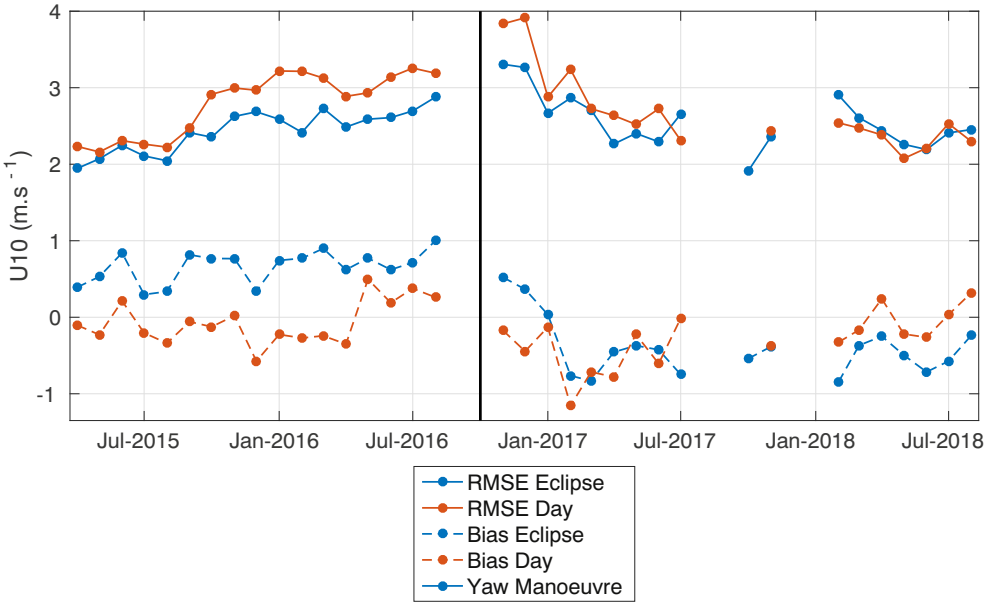


**Fig. 3.** Time series of the TDS-1 wind speed bias (dotted lines) and RMSE (solid lines) calculated monthly against ERA5 for TDS-1 data obtained in daylight (orange) and eclipse (blue) conditions. TDS-1 wind speed is computed using the NOC C-BRE v0.5 algorithm. The vertical black line marks the time in October 2016 when the TDS-1 satellite was rotated 180° in yaw. Note the changes in RMSE and bias before and after the yaw manoeuvre and the improved consistency between daylight and eclipse data after October 2016. (For interpretation of the references to colour in this figure legend, the reader is referred to the web version of this article.)

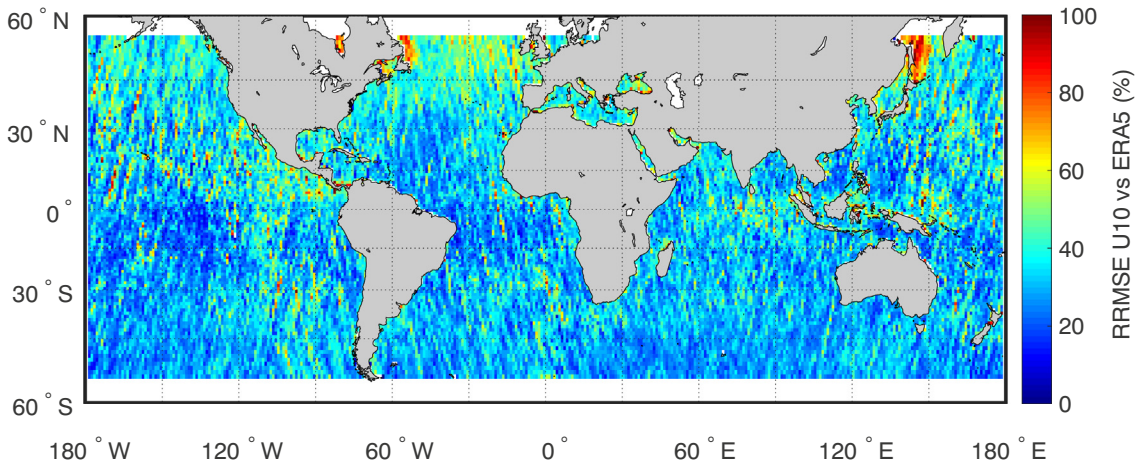


**Fig. 4.** Global 1° gridded map of Relative Root Mean Square Error (RRMSE) of TDS-1 wind speed (NOC C-BRE v0.5) computed against ERA5 over the entire PGM phase of the mission (April 2015 – August 2018). RRMSE is calculated as the RMSE divided by the average ERA5 wind speed in each grid cell, and represents a performance indicator independent of wind speed.

compared to ERA5 estimates. This effect is most likely attributable to the occasional presence of sea-ice providing strong reflections that are unfiltered by the current time-invariant latitudinal mask (55S–55N). Further improvements of the algorithm should aim to include improved filtering and flagging mechanisms for sea-ice, based either on ancillary data, or on the GNSS-R waveform (e.g. Yan and Huang, 2016b; Alonso-Arroyo et al., 2017).

## 4. Discussion: effects of attitude and transmit power changes on wind speed retrieval performance

### *4.1. Effects of GPS transmitter power changes on wind speed retrieval performance*

Reduced wind speed retrieval performance at high northern latitudes seems to be attributable to certain groups of GPS transmitters. By removing blocks IIR-M and IIF the decrease in performance seen in the North Atlantic and North Pacific is mostly resolved (Fig. 6). This likely results from specific events where transmit power is changed at certain times and sometimes for certain spatial regions, that have been described as GPS Flex modes by Steigenberger et al. (2019). Fig. 7 shows the geographical effect on wind speed retrieval of one of these changes in Block IIF transmit power, resulting in a well-defined area of negative bias in wind speed (the result of increased transmit power) after January 2017, which was not visible before this time. These wind speed biases are seen in the North Atlantic, northern Indian Ocean, the Mediterranean, the Black Sea, and the Sea of Okhotsk and reach up to 3 $m{\cdot}s^{-1}$. The change in transmitter power of GPS Block IIF satellites in January 2017 may also explain part of the shift in wind speed retrieval bias seen in Fig. 3 from around this time. Steigenberger et al. (2019) also report another geographical flex mode centred on the North Pacific for three 11 h periods during April/May 2018. However, no evidence is found in the TDS-1 data of this geographical Flex mode, possibly due to the short duration of the event and the limited number of TDS-1 passes during this time.

The C-BRE v0.5 algorithm includes empirical corrections that mitigate differences in direct signal power between GPS transmitters. However, in this version of the algorithm, these corrections are computed only once for the whole mission and are therefore time and space invariant. Future versions of the C-BRE algorithm will aim to include additional mitigation mechanisms to also address spatio-temporal variability of transmitted GPS power.

### *4.2. Effects of attitude on wind performance*

TDS-1 has a nominal attitude of 0°/0°/0° (in roll/pitch/yaw) prior to the yaw manoeuvre in October 2016 when the nominal yaw becomes 180°, however some variability around nominal orientation has been reported by the on-board attitude system (Foti et al., 2017b). To investigate the impact of attitude performance on C-BRE wind speed retrieval the standard deviation of reported platform orientation (roll, pitch, yaw, and overall magnitude) are plotted in Fig. 8. These results

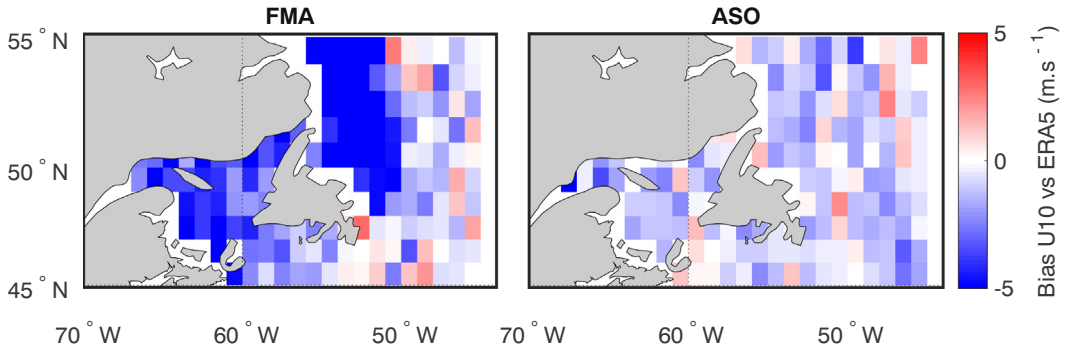


**Fig. 5.** Climatological maps of 1° gridded TDS-1 wind speed bias over the Labrador Sea against ERA5 for two seasonal periods: (left) February – April and (right) August – October. TDS-1 wind speed is computed using the NOC C-BRE v0.5 algorithm. The two periods represent the maximum and minimum seasonal sea-ice extents, respectively. Note the large area of negative bias close to land in the February – April period caused by the lack of sea ice flag in C-BRE v0.5, meaning that signals reflected over sea-ice are confused for low wind speeds.

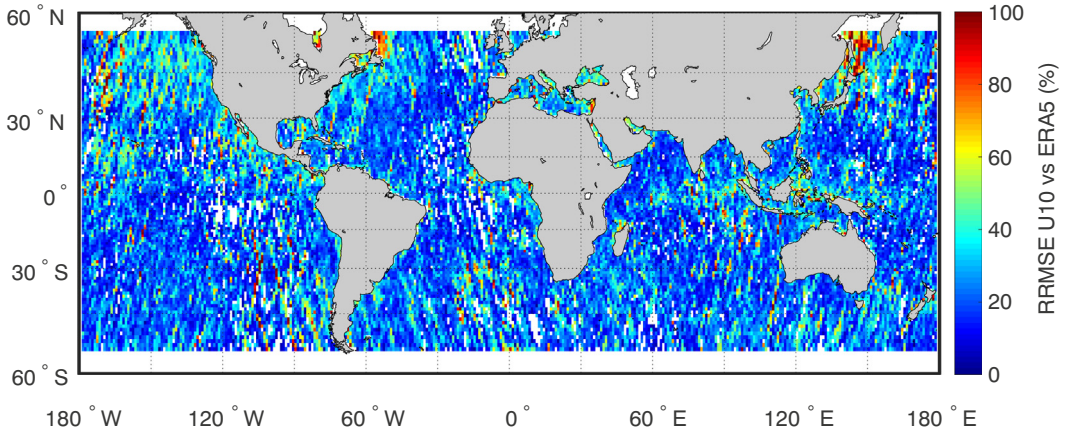


**Fig. 6.** Global 1° gridded map of Relative Root Mean Square Error (RRMSE) of TDS-1 wind speed (NOC C-BRE v0.5) computed against ERA5 over the entire PGM phase of the mission (April 2015 – August 2018) but excluding all data transmitted by Block IIF or Block IIR-M GPS satellites.

show that there are clear changes in the stability of platform attitude over time. Fig. 9 shows the temporal evolution of standard deviation of roll, plotted on the same timescale as RMSE of the C-BRE algorithm vs ERA5. A clear similarity is found in the temporal evolution of the two parameters, suggesting the presence of a direct link between platform attitude performance and wind speed retrieval performance.

To further assess the dependence of wind speed retrieval performance on attitude uncertainty, a sensitivity analysis is performed using a series of statistical simulations. Fluctuations in satellite attitude will affect the antenna gain at the specular point as observed by the receiver. Since the antenna gain at the specular point is required in the C-BRE inversion, attitude errors will thus introduce errors in the retrieved wind speed. Statistical simulations were set up so that different levels of additional random attitude fluctuations are introduced prior to the estimation of the antenna gain at the specular point and the computation of C-BRE wind speeds. For each statistical simulation, 100 samples are drawn randomly from 19 normal distributions for each of roll, pitch, and yaw; the attitude distributions are assumed to have means equal to zero (unbiased) and have standard deviations that increase from 0° to 10°, using 0.2° steps between 0° and 2° and 1° steps between 2° and 10°, representing increasing attitude uncertainty. The simulations are applied to real TDS-1 data taken from two separate months, using only data points where valid wind speeds can be retrieved. The two selected months are May 2015, when wind speed retrieval performance is at its best (~ 2 $m{\cdot}s^{-1}$) and May 2016 when retrieval performance is significantly worse (Fig. 3). For each simulation, the performance of the re-calculated C-BRE wind speeds is assessed against collocated ERA5 data using RMSE as a metric.

The results of these analyses are shown in Fig. 10. They confirm that RMSE in May 2015 (blue curve) is better than in May 2016 (orange curve), with results for X = 0 (i.e. no added attitude fluctuations) reproducing the RMSE found for TDS-1 in these months in Fig. 3. For both

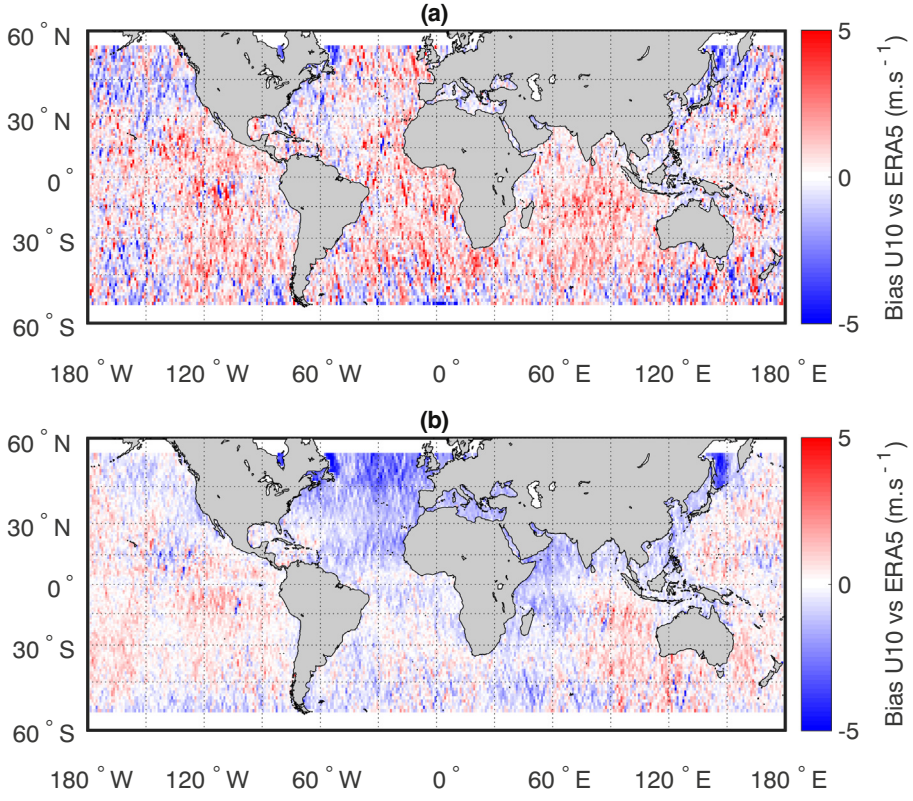


**Fig. 7.** Global maps of 1° gridded TDS-1 wind speed bias computed against ERA5 in (a) April 2015 – January 2017 and (b) February 2017 – August 2018, showing the appearance of a large region of negative wind speed bias after January 2017 over the North Atlantic, northern Indian Ocean, the Mediterranean Sea, and the Sea of Okhotsk.

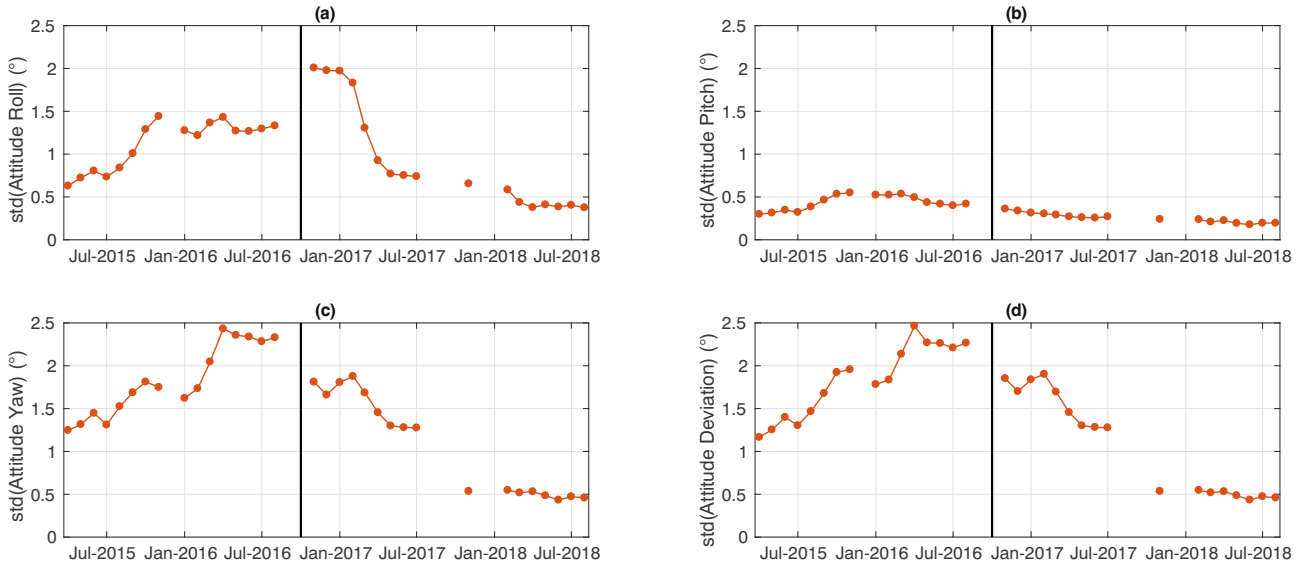


**Fig. 8.** Temporal evolution of TDS-1 attitude fluctuations shown as the standard deviation of measurements of (a) roll, (b) pitch, (c) yaw, and (d) the vector norm of these three attitude parameters. The vertical black line marks the time in October 2016 when TDS-1 satellite was rotated 180° in yaw. All parameters, except pitch, show significant changes over time.

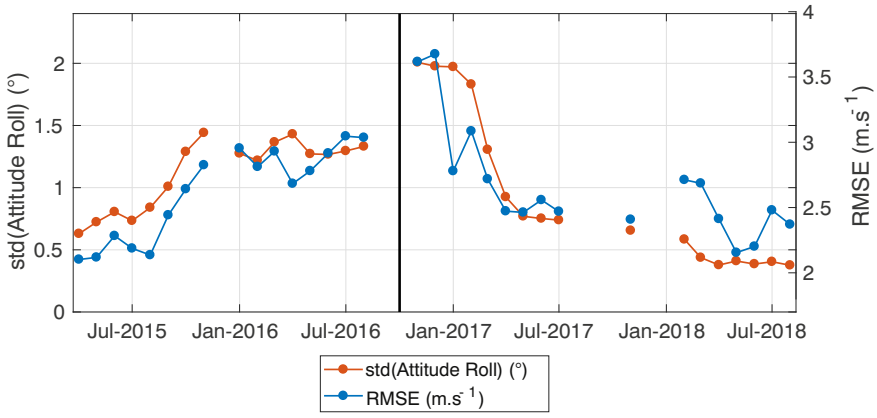


**Fig. 9.** Temporal evolution of TDS-1 roll fluctuations (orange) and TDS-1 wind speed RMSE against ERA5 (blue). The vertical black line marks the time in October 2016 when TDS-1 satellite was rotated 180° in yaw. The two variables show very similar temporal evolutions suggesting a close link between wind retrieval performance and platform attitude. (For interpretation of the references to colour in this figure legend, the reader is referred to the web version of this article.)

months, there is a clear degradation of the wind retrieval performance (RMSE) as attitude uncertainty increases (represented on the x-axis by the standard deviation of the added attitude fluctuations). This is due to the effect of increasingly large errors in the estimated antenna gain at the specular point. Results indicate that a 4° increase in TDS-1 attitude uncertainty results in a 0.7–1 $m{\cdot}s^{-1}$ increase in wind speed RMSE. Note that this estimated sensitivity of wind performance to attitude is only approximate since the response is non-linear (Fig. 10). The data in May 2016 present significantly worse performance than in May 2015, with results implying that TDS-1 was subject to nearly 3° of additional attitude standard deviation in May 2016 compared to May 2015. At the same time, the on-board sensor data (Fig. 8d) report a mere 1° increase in the TDS-1 attitude standard deviation between May 2015 and May 2016, suggesting that the reported attitude data significantly underestimate the true magnitude of platform attitude fluctuations.

As the nadir antenna on TDS-1 is highly directional, with prominent anisotropy and steep gradients away from the main beam, even small uncertainties in attitude knowledge can propagate into large errors in antenna gain at the specular point, especially for specular points with high incidence angles. Based on these results, it is clear that accurate attitude knowledge and a well-characterised antenna pattern should be prioritised for future GNSS-R missions. Our results indicate that TDS-1 attitude data do not fully reflect real platform attitude, so that even the best wind speed retrieval performance reported for TDS-1 in May 2015 could still include error contributions linked to uncorrected satellite attitude effects. As it stands, uncertainties in the nadir antenna gain map and the absence of reliable attitude knowledge on TDS-1 limits the ability to further determine the achievable wind speed inversion performance of the NOC C-BRE algorithm for GNSS-R signals from TDS-1.

## 5. Conclusions and recommendations

This paper analyses wind speed retrieval performance of the NOC C-BRE v0.5 algorithm across the entire lifespan of the TDS-1 mission compared to ECMWF ERA5 reanalysis wind data. Inversion accuracy is shown to be generally good, with similar global distributions to ERA5, albeit with slight overestimation of the highest speed winds and underestimation of the lower winds. However, inversion performance is found to be a) markedly different in the sunlit and eclipsed portions of the orbit, b) significantly worse in sunlight, and c) temporally evolving in a similar way to attitude performance, with increasing attitude degradation corresponding to a decrease in retrieval accuracy. Additional factors (other than platform attitude) might also be playing a significant role in the retrieval process, including spatio-temporal changes in transmitted GPS signal power.

Man-made changes in GPS signal power levels are generally not made available to the public, but some have been reported in the literature, which have the potential to significantly affect the wind

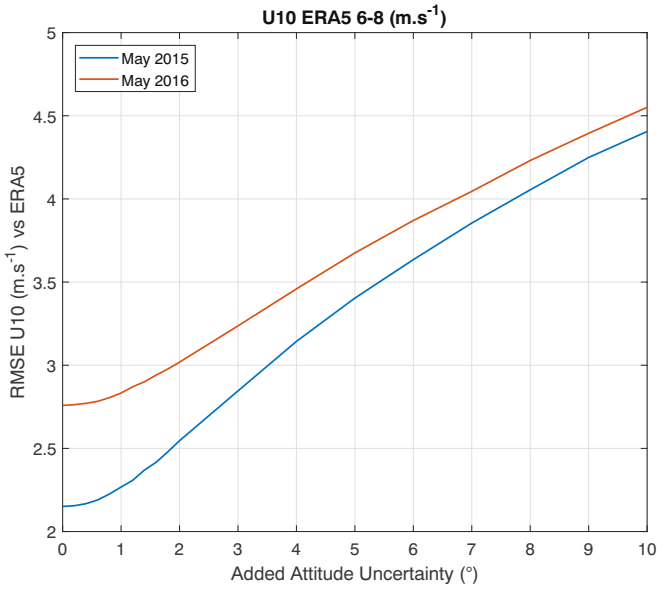


**Fig. 10.** Results of statistical simulations showing the relationship between TDS-1 wind speed performance (RMSE against ERA5) and platform attitude uncertainty (attitude standard deviation) for a period of good TDS-1 performance (May 2015; blue) and a period of poorer performance (May 2016; orange). See text in Section 4.2 for details. (For interpretation of the references to colour in this figure legend, the reader is referred to the web version of this article.)

retrieval inversion. These changes have been shown to occur in specific regions of the globe, and sometimes only for specific time periods (Steigenberger et al., 2019), and can bias retrieved wind speeds by up to 3 $m{\cdot}s^{-1}$.

These findings lead to some important general recommendations for future GNSS-R missions in order to achieve more consistent and robust inversion performance:

- High-quality platform attitude knowledge data should be an absolute priority to ensure the location of the specular point in the antenna footprint can be accurately determined, and with it, the antenna gain at the specular point.
- GNSS-R nadir antenna gain patterns should be well characterised before launch, preferably after integration on the satellite, to reduce errors in the estimated antenna gain at specular points.
- Variations in transmitted GPS power levels, due to hardware evolution or deliberate programmed (and not always publicised) changes need to be taken into account to achieve geographically consistent and temporally stable retrievals. More effort is needed to develop strategies to address this issue, based on onboard sensor data or other methods.

This paper highlights that global realistic retrievals of ocean wind speed can be achieved from spaceborne altitudes using GNSS-R. At the same time, the prominent role of platform attitude knowledge in the inversion error budget has been demonstrated. However, further work is still needed to address other possible contaminating factors, including the spatio-temporal variability of GNSS direct signal power.

## CRediT authorship contribution statement

**Matthew Lee Hammond:**Investigation, Software, Visualization, Writing - original draft, Writing - review & editing.**Giuseppe Foti:**Conceptualization, Software, Supervision, Writing - review & editing.**Christine Gommenginger:**Conceptualization, Supervision, Writing - review & editing.**Meric Srokosz:**Conceptualization, Supervision, Writing - review & editing.

## Declaration of competing interest

The authors declare that they have no known competing financial interests or personal relationships that could have appeared to influence the work reported in this paper.

## Acknowledgements

ERA5 data was generated using Copernicus Climate Change Service Information [2018] neither the European Commission nor ECMWF is responsible for any use that may be made of the Copernicus Information or Data it contains. Data from TDS-1 and the NOC C-BRE v0.5 wind speed data are made available by SSTL & NOC at www.merrbys.co.uk. This work was funded by the ESA contract 4000123436/NL/FF/gp. G.F. was supported by NERC grant no. NE/N018095/1 (Ocean Regulation of Climate by Heat and Carbon Sequestration and Transports, ORCHESTRA).

## References

Alonso-Arroyo, A., Zavorotny, V.U., Camps, A., 2017. Sea ice detection using U.K. TDS-1 GNSS-R data. IEEE Trans. Geosci. Remote Sens. 55 (9), 4989–5001. https://doi.org/10.1109/TGRS.2017.2699122.

Asgarimehr, M., Wickert, J., Reich, S., 2018. TDS-1 GNSS Reflectometry: development and validation of forward scattering winds. IEEE Journal of Selected Topics in Applied Earth Observations and Remote Sensing 11 (11), 4534–4541. https://doi.org/10.1109/JSTARS.2018.2873241.

Belmonte Rivas, M., Stoffelen, A., 2019. Characterizing ERA-interim and ERA5 surface wind biases using ASCAT. In: Ocean Science Discussions, pp. 1–31. https://doi.org/10.5194/os-2018-160. January.

Camps, A., Vallossera, M., Park, H., Portal, G., Rossato, L., 2018. Sensitivity of TDS-1 GNSS-R reflectivity to soil moisture: global and regional differences and impact of different spatial scales. Remote Sens. 10 (11). https://doi.org/10.3390/rs10111856.

Carreno-Luengo, H., Camps, A., Via, P., Munoz, J.F., Cortiella, A., Vidal, D., ... Cornara, S., 2016. 3Cat-2-An Experimental nanosatellite for GNSS-R Earth Observation: mission Concept and Analysis. IEEE Journal of Selected Topics in Applied Earth Observations and Remote Sensing 9 (10), 4540–4551. https://doi.org/10.1109/JSTARS.2016.2574717.

Cartwright, J., Clarizia, M.P., Cipollini, P., Banks, C., Srokosz, M., 2018. Independent DEM of Antarctica using GNSS-R data from TechDemoSat-1. Geophys. Res. Lett. https://doi.org/10.1029/2018GL077429.

Egido, A., Paloscia, S., Motte, E., Guerriero, L., Pierdicca, N., Caparrini, M., Floury, N., 2014. Airborne GNSS-R polarimetric measurements for soil moisture and above-ground biomass estimation. IEEE Journal of Selected Topics in Applied Earth Observations and Remote Sensing 7 (5), 1522–1532. https://doi.org/10.1109/JSTARS.2014.2322854.

Foti, G., Gommenginger, C., Jales, P., Unwin, M., Shaw, A., Robertson, C., Rosello, J., 2015. Spaceborne GNSS reflectometry for ocean winds: first results from the UK TechDemoSat-1 mission. Geophys. Res. Lett. 42 (13), 5435–5441. https://doi.org/10.1002/2015GL064204.

Foti, G., Gommenginger, C., Srokosz, M., 2017a. First Spaceborne GNSS-Reflectometry observations of hurricanes from the UK TechDemoSat-1 mission. Geophys. Res. Lett. 44 (24), 12,358–12,366. https://doi.org/10.1002/2017GL076166.

Foti, G., Gommenginger, C., Unwin, M., Jales, P., Tye, J., Rosello, J., 2017b. An assessment of non-geophysical effects in spaceborne GNSS reflectometry data from the UK techdemosat-1 mission. IEEE Journal of Selected Topics in Applied Earth Observations and Remote Sensing 10 (7), 3418–3429. https://doi.org/10.1109/JSTARS.2017.2674305.

Gleason, S., 2006. Sensing Ocean, Ice and Land Reflected Signals From Space: Results from the UK-DMC GPS Reflectometry Experiment. University of Surrey, U.K.

Gleason, S., Gebre-Egziabher, D., 2009. GNSS Applications and Methods. Artech House, Boston, Mass.

Hall, C.D., Cordey, R.A., 1988. Multistatic scatterometry. International geoscience and remote sensing symposium. In: Remote Sensing: Moving Toward the 21st Century, https://doi.org/10.1109/IGARSS.1988.570200.

Hersbach, H., De Rosnay, P., Bell, B., Schepers, D., Simmons, A., Soci, C., Zuo, H., 2018. Operational global reanalysis: progress, future directions and synergies with NWP including updates on the ERA5 production status. In: ERA Report Series No. 27, 27 (8th October), pp. 1–63. https://doi.org/10.21957/tkic6g3wm.

Jales, P., Unwin, M., 2015. ESA TDS-1 GNSS-R Exploitation Study. Surrey Satellite Technology Ltd, 1. Retrieved from. http://merrbys.co.uk/wp-content/uploads/2017/07/TDS-1-GNSS-R-Mission-Description.pdf.

Katzberg, S.J., Torres, O., Ganoe, G., 2006. Calibration of reflected GPS for tropical storm wind speed retrievals. Geophys. Res. Lett. 33 (18), 1–5. https://doi.org/10.1029/2006GL026825.

Komjathy, A., Maslanik, J., Zavorotny, V.U., Axelrad, P., Katzberg, S.J., 2000. Sea ice remote sensing using surface reflected GPS signals. In: IGARSS 2000. IEEE 2000

International Geoscience and Remote Sensing Symposium. Taking the Pulse of the Planet: The Role of Remote Sensing in Managing the Environment. Proceedings (Cat. No. 00CH37120). 7. pp. 2855–2857. https://doi.org/10.1109/IGARSS.2000.860270.

Komjathy, A., Armatys, M., Masters, D., Axelrad, P., Zavorotny, V., Katzberg, S., 2004. Retrieval of ocean surface wind speed and wind direction using reflected GPS signals. J. Atmos. Ocean. Technol. 21 (3), 515–526. https://doi.org/10.1175/1520-0426(2004)021<0515:ROOSWS>2.0.CO;2.

Li, W., Cardellach, E., Fabra, F., Ribó, S., Rius, A., 2018. Lake level and surface topography measured with spaceborne GNSS-Reflectometry from CYGNSS mission: example for the Lake Qinghai. Geophys. Res. Lett. 45 (24), 13,332–13,341. https://doi.org/10.1029/2018GL080976.

Masters, D., Zavorotny, V., Katzberg, S., Emery, W., 2000. GPS signal scattering from land for moisture content determination. In: IGARSS 2000. IEEE 2000 International Geoscience and Remote Sensing Symposium. Taking the Pulse of the Planet: The Role of Remote Sensing in Managing the Environment. Proceedings (Cat. No. 00CH37120). 7. pp. 3090–3092. https://doi.org/10.1109/IGARSS.2000.860346.

Soisuvarn, S., Jelenak, Z., Said, F., Chang, P.S., Egido, A., 2016. The GNSS Reflectometry response to the ocean surface winds and waves. IEEE Journal of Selected Topics in Applied Earth Observations and Remote Sensing 9 (10), 4678–4699. https://doi.org/10.1109/JSTARS.2016.2602703.

Steigenberger, P., Thölert, S., Montenbruck, O., 2019. Flex power on GPS block IIR-M and IIF. GPS Solutions 23 (1), 1–12. https://doi.org/10.1007/s10291-018-0797-8.

Valencia, E., Camps, A., Park, H., Rodriguez-Alvarez, N., Bosch-Lluis, X., Ramos-Perez, I., 2011. Oil slicks detection using GNSS-R. International Geoscience and Remote Sensing Symposium (IGARSS), 2(1) 4383–4386. https://doi.org/10.1109/IGARSS.2011.6050203.

Yan, Q., Huang, W., 2016a. Tsunami detection and parameter estimation from GNSS-R delay Doppler maps. IEEE Journal of Selected Topics in Applied Earth Observations and Remote Sensing 9 (10), 4650–4659. https://doi.org/10.1109/JSTARS.2016.2524990.

Yan, Q., Huang, W., 2016b. Spaceborne GNSS-R sea ice detection using delay-Doppler maps: first results from the U.K. TechDemoSat-1 mission. IEEE Journal of Selected Topics in Applied Earth Observations and Remote Sensing 9 (10), 4795–4801. https://doi.org/10.1109/JSTARS.2016.2582690.

Zavorotny, V.U., Gleason, S., Cardellach, E., Camps, A., 2014. Tutorial on remote sensing using GNSS bistatic radar of opportunity. IEEE Geoscience and Remote Sensing Magazine 2 (4), 8–45. https://doi.org/10.1109/MGRS.2014.2374220.